Advanced PID Control

Karl J. Åström Tore Hägglund

Department of Automatic Control
Lund Institute of Technology
Lund University

ISA–The Instrumentation, Systems, and Automation Society

8

Predictive Control

8.1 Introduction

A PI controller only considers present and past data, and a PID controller also predicts the future process behavior by linear extrapolation. There have been many attempts to find other ways of predicting future process behavior and to take this into account when making the control actions. Good predictions can improve controller performance, particularly when the process has time delays, which are common in process control. Time delays can arise from a pure delay mechanism caused by transport or time for computation and communication. Delays may also be caused by measurements obtained by off-line analysis. They also appear when a high-order system or a partial differential equation is approximated with a low-order model as in heat conduction. Time delays appear in many of the models discussed in this book. A new controller that could deal with processes having long time delays was proposed by Smith in 1957. The controller is now commonly known as the Smith predictor. It can be viewed as a new type of controller but it can also be interpreted as an augmentation of a PID controller. There are also many other controllers that have predictive abilities. The model predictive controller is a large class of controller that is becoming increasingly popular.

In this chapter we start by presenting the Smith predictor in Section 8.2. This controller can give significant improvements in the response to set-point changes, but the Smith predictor can also be very sensitive to model uncertainties. This is shown in Section 8.3 where we analyze the closed-loop system when a Smith predictor is used. The analysis also shows that the concepts of gain and phase margin are not sufficient to characterize the robustness of the system. The reason for this is that the Nyquist curve of the loop transfer function can have large loops at frequencies larger than the gain crossover frequency. The robustness is well captured by the properties of the *Gang of Four*, and there is also another classical robustness measure, the delay margin, that gives good insight. A special type of the Smith predictor called the PPI controller is discussed in Section 8.4. This controller is simpler and more robust. Model predictive control, a more general form of prediction that is gaining in popularity, is discussed in Section 8.6.

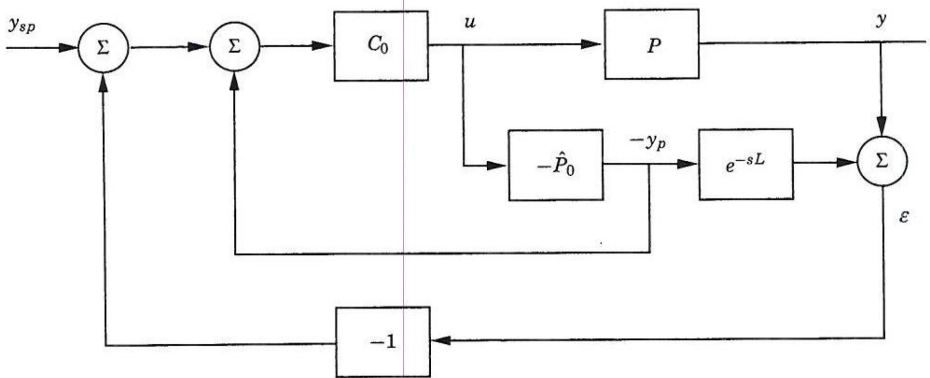

Figure 8.1 Block diagram of a system with a Smith predictor.

8.2 The Smith Predictor

To describe the idea of a Smith predictor we consider a process with a time delay L, and we factor the process transfer function as

$$P(s) = P_0(s)e^{-sL}, \tag{8.1}$$

where the transfer function P_0 does not have any time delays. Figure 8.1 shows a block diagram of a closed-loop system with a Smith predictor. The controller consists of an ordinary PI or PID controller C_0 and a model of the process $\hat{P}$, factored in the same way as the process, connected in parallel with the process. If the model is identical with the process the signal y_p represents the output without the delay or, equivalently, a prediction of what the output would be if there were no delays. By using the model it is thus possible to generate a prediction of the output. The signal y_p is fed back to the controller, and there is also an additional feedback from the process output y to cope with load disturbances. If the model $\hat{P}$ is identical to the process P and if there are no disturbances acting on the process the signal ε is zero. This means that the outer feedback loop gives no contribution, and the input-output relation of the system is given by

$$G_{yy_{sp}} = \frac{PC_0}{1+P_0C_0} = \frac{P_0C_0}{1+P_0C_0}e^{-sL}. \tag{8.2}$$

The controller C_0 can thus be designed as if the process has no time delay, and the response of the closed-loop system will simply have an additional time delay.

The system shown in Figure 8.1 can also be represented by the block diagram in Figure 8.2, which is an ordinary feedback loop with a process P and a controller C, where the controller has the transfer function

$$C = \frac{C_0}{1+C_0(\hat{P}_0 - \hat{P})} = \frac{C_0}{1+C_0\hat{P}_0(1-e^{-sL})}. \tag{8.3}$$

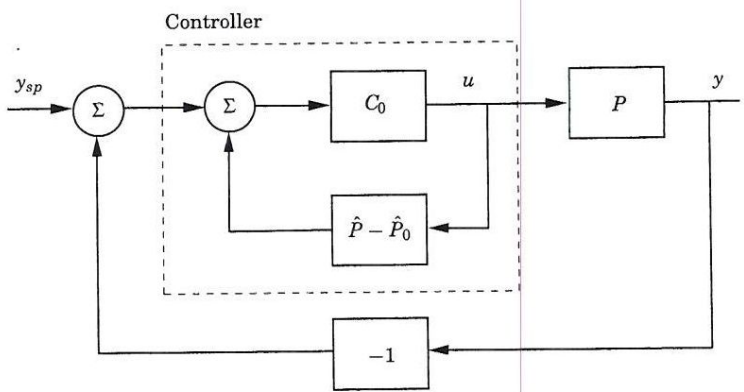

Figure 8.2 Another representation of a system with a Smith predictor.

The transfer function $\hat{P}_0 e^{-sL}$ is the transfer function of the process model used to design the controller. The controller C is thus obtained by wrapping a feedback around the controller C_0. The input-output relation of the controller C can be written as

$$U(s) = C_0(s)\big(E(s) - \hat{P}_0(s)(1 - e^{-sL})U(s)\big), \tag{8.4}$$

where $U(s)$ and $E(s)$ are the Laplace transforms of the control signal and the error. The term $\hat{P}_0(s)(1 - e^{-sL})U(s)$ can be interpreted physically as the predicted effect on the output of control signals in the interval $(t - L, t)$. The Smith predictor can thus be interpreted as an ordinary PI controller where the effects of past control actions are subtracted from the error. The controller can be compared with a PID controller, which predicts by extrapolating the current process output linearly, as is illustrated in Figure 3.5. This type of prediction is less effective for systems with time delays because future process outputs are strongly influenced by past control control actions rather than current inputs.

The properties of the Smith predictor will be illustrated by an example.

EXAMPLE 8.1—FIRST-ORDER SYSTEM WITH TIME DELAY
Consider a process with transfer function

$$P(s) = \frac{K_p}{1 + sT} e^{-sL}. \tag{8.5}$$

A PI controller that gives the characteristic polynomial

$$s^2 + 2\zeta\omega_0 s + \omega_0^2$$

for the process without delay is designed as described in Section 6.4. The controller is

$$C_0(s) = K\Big(1 + \frac{1}{sT_i}\Big),$$

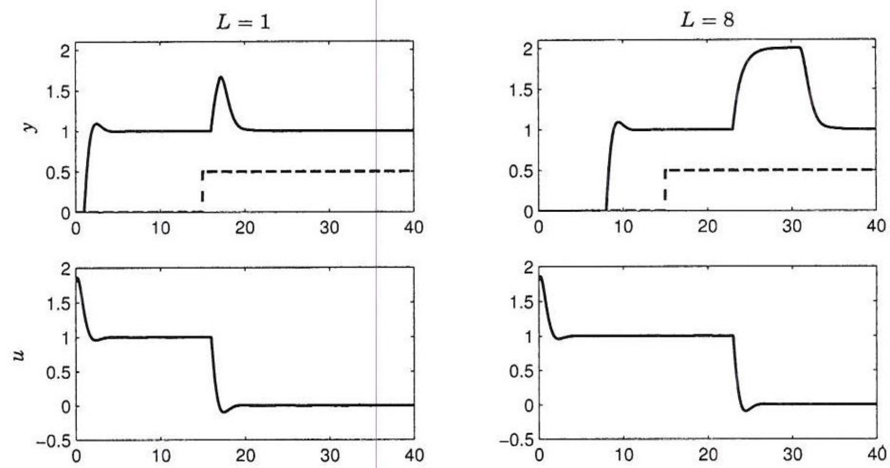

Figure 8.3 Responses of a closed-loop system with Smith predictor. The process has the transfer function $P(s) = e^{-sL}/(s+1)$, and the figure shows response for $L = 1$ and 8. The dashed line is the load disturbance.

where

$$
\begin{aligned}
K &= \frac{2\zeta\omega_0 T - 1}{K_p} \\
T_i &= \frac{K_p K}{\omega_0^2 T}.
\end{aligned}
\tag{8.6}
$$

Figure 8.3 shows the responses of the system to a unit step change in the set point and a load disturbance in the form of a unit step in the process input. The load disturbance is applied at time $t = 15$ in all cases. The time constant is equal to one in all cases, and the time delay L is changed. The PI controller is designed to give a closed-loop system with $\omega_0 = 2$ and $\zeta = 0.7$ for the process without delays. The figure shows that the responses to set point have the same shape but with a delay that changes with the process delay. The shape is the same as for a system without the time delay. This property of the system is quite remarkable.

The shapes of the responses to load disturbances change with the time delay L. With increasing time delay it will take a longer time for the system to react. The initial part of the responses are similar but with different delays. Because of the varying delay the time to recover from the disturbance varies with the time delay. □

Analyzing the results it may appear remarkable that it is possible to obtain such good responses even when the time delay is as long as $L = 8$. In the following we will analyze the systems obtained when using the Smith's predictor to better understand its behavior.

The Predictor

It follows from (8.3) that the Smith predictor can be viewed as the cascade connection of an ordinary controller C_0 and a block with the transfer function

$$C_{pred} = \frac{1}{1 + C_0(\hat{P}_0 - \hat{P})} = \frac{1}{1 + C_0\hat{P}_0(1 - e^{-sL})}. \tag{8.7}$$

To obtain the responses shown in Figure 8.3 the transfer function C_{pred} compensates for the time delay of the process. Intuitively this can be understood in the following way. Assume $C_0\hat{P}_0 \approx -1$; it then follows from (8.7) that

$$C_{pred} \approx e^{sL}.$$

This means that the transfer function $C_{pred}(s)$ acts like an ideal predictor. We can therefore expect that the transfer function C_{pred} behaves like an ideal predictor for frequencies where $C_0(i\omega)\hat{P}_0(i\omega)$ is close to -1. Notice that it is not possible to have $C_0(i\omega)\hat{P}_0(i\omega) = -1$ for any frequency because the transfer function (8.2) is then unstable. The properties of the transfer function (8.7) will be illustrated by an example.

EXAMPLE 8.2—PREDICTOR FOR FIRST-ORDER SYSTEM WITH TIME DELAY
Consider the same system as in Example 8.1. Assuming that there are no modeling errors it follows that $\hat{P} = P = P_0e^{-sL}$. Combined with a PI controller the predictor becomes

$$C_{pred} = \frac{1}{1 + C_0(P_0 - P)} = \frac{1}{1 + \dfrac{K_pK(1 + sT_i)}{sT_i(1 + sT)}(1 - e^{-sL})}. \tag{8.8}$$

It follows from (8.8) that $C_{pred}(i\omega) = 1$ for $\omega L = 2\pi, 4\pi, 6\pi, \ldots$ and that $C_{pred}(s)$ goes to 1 for large s. The transfer function C_{pred} has the series expansion

$$C_{pred}(s) = \frac{T_i}{T_i + K_pKL}\Big(1 + \frac{K_pKL}{T_i + K_pKL}(T + \frac{L}{2} - T_i)s + \ldots\Big).$$

The static gain of C_{pred} decreases with increasing L and is always less than one. Figure 8.4 shows the Bode plot for the transfer function for $L = 8$. The figure shows that the transfer function gives a very large phase advance, more than 800°. A comparison with the phase curve of an ideal predictor shows that the system does approximate an ideal predictor well for certain frequencies. The solid and dashed curves are very close for those frequencies where the gain curve has peaks. Notice, however, that the gain curves are different. The ideal predictor has constant gain, but the gain of the transfer function C_{pred} changes with several orders of magnitude.

We will now investigate how the large phase advance is created. Figure 8.5 shows Nyquist curves of the transfer function C_{pred} for $K_p = 1$, $T = 1$, $K = 1.8$, $T_i = 0.45$, and $L = 1$, 2.5, 4, and 8. For $L = 1$ the largest phase advance is close to 90°. The phase advance increases with increasing L, as is indicated in the curve for $L = 2.5$ where the circular part of the Nyquist curve increases. The Nyquist curve goes to infinity for $L = 2.99$, which indicates that the

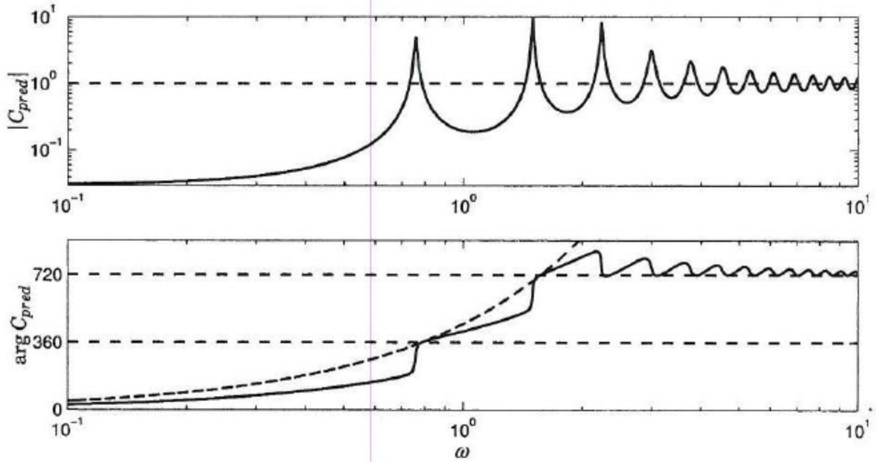

Figure 8.4 Bode plot of the loop transfer functions $C_{pred}(s)$ given by (8.8) for $L = 8$ (solid) and for the ideal predictor e^{sL} (dashed).

transfer function has poles on the imaginary axis. For larger L the Nyquist curve encircles the origin, which means that the phase advance is more than 360°. The curve for $L = 4$ shows that the largest phase advance is more than 450°. As L is increased further the Nyquist curve again goes to infinity for $L = 6.40$, and for larger L there are two encirclements of the origin, indicating that the phase advance is more than 720°. The curve for $L = 8$ shows that the largest phase advance is more than 800°.

To deform the curve for $L = 2.5$ continuously to the curve for $L = 4$ in Figure 8.5 the curve must go to infinity for some intermediate value of L. In the particular case the Nyquist curve of C_{pred} goes to infinity for $L = 2.99$, 6.40, 9.80, 13.40, 17,00, 20.6, ... This means that the transfer function C_{pred} is unstable for some values of L. It has two poles in the right-half plane for $2.99 < L < 6.40$, four poles in the right half plane for $6.40 < L < 9.80$, etc. For the simulation with $L = 10$ in Figure 8.3 the predictor transfer function has six poles in the right half plane. The predictor (8.3) thus achieves very large phase advances through poles in the right half plane. □

There are severe drawbacks with unstable controllers. It follows from Bode's integral (4.28) that poles in the right half plane increase the sensitivity. The remarkable response to set-point changes shown in Figure 8.3 thus comes at a price. Some of these issues will be discussed in the next section.

[redacted]